Available online at www.sciencedirect.com

ScienceDirect

Energy Procedia 126 (201709) 1043–1050

Energy Procedia

www.elsevier.com/locate/procedia

72nd Conference of the Italian Thermal Machines Engineering Association, ATI2017, 6–8 September 2017, Lecce, Italy

Numerical Simulations of the flow field and chemical reactions of the Storage/Oxidation process within a NSC *Pt – BaO* Catalyst

Francesco Fornarelli[a,*], Ruggiero Dadduzio[a], Marco Torresi[a], Sergio Mario Camporeale[a], Bernardo Fortunato[a]

[a] *Politecnico di Bari, Dipartimento di Meccanica, Matematica e Management, Bari, Italy*

Abstract

A NO_x Storage Catalyst (NSC) has been studied by means of reactive CFD simulations. In the scenario of automotive pollutant emission reduction, due to the stringent regulation, the detailed description of the chemical and physical phenomena within catalysts represents a key point in order to improve their conversion efficiency. The active part of the catalyst has been simulated as a porous medium. In this zone, surface reactions take place, which are modelled by means of an Arrhenius chemical kinetic approach, involving the *Pt* and *BaO* sites on the active surface of the matrix. Actually, two chemical mechanisms are considered, the simplest involves only *BaO* site, the other one includes both *BaO* and *Pt* sites. Both models are validated against data available in the literature and then applied to a real automotive catalyst geometry. Thus, a detailed description of the spatial distribution of the species is provided for both models. Lean condition is simulated in order to check the catalyst behaviour according to experimental results.

Peer-review under responsibility of the scientific committee of the 72nd Conference of the Italian Thermal Machines Engineering Association

Keywords: NO_x storage, kinetic modelling, catalyst, CFD

1. Introduction

The serious situation on air pollution sets more stringent rule for emissions of diesel engines moving the attention of the scientific community towards more detailed analyses in order to optimize the behaviour of exhaust after-treatment systems for NO_x abatement. Typical aftertreatment devices able to reduce the NO_x emissions in diesel combustion engines are the Selective Catalyst Reduction (SCR) systems and the Nitrogen oxide Storage Catalysts (NSC) also known as Lean NO_x Traps (LNT). The first ones permit the NO_x reduction to N_2 by means of an injection of an urea solution in the exhaust gas. LNT systems operate normally under excess of oxygen, absorbing NO_x into the washcoat consisting of alkaline earth or alkali metal such as ceria (CeO_2) or barium-oxide (BaO): the subsequent regeneration

* Corresponding author. Tel.: +390805963627 ; fax: +39 080 596 3411.
E-mail address: francesco.fornarelli@poliba.it.

1876-6102
Peer-review under responsibility of the scientific committee of the 72nd Conference of the Italian Thermal Machines Engineering Association
10.1016/j.egypro.2017.08.311

phase occurs thanks to periodic short rich combustion, which promote the NO_x release as molecular N_2. The analysis of the catalyst behaviour, involves several phenomena including both chemical and physical variables. Often, the modelling of catalyst is based on 0-1D plug flow reactor (PFR) codes, because of the short computational time required, tuning the kinetic reaction rates on experimental results. There are examples of very complicated microkinetic detailed mechanisms for the description of the chemical process in simplified LNT monoliths [1] [2]. They include a large number of species and reactions in order to take into account the different operative working conditions of the engine. Benjamin et al. [3] made CFD simulations on a simplified geometry reproducing a real automotive catalyst with a porous medium approach for the modellization of the catalytic matrix and used a simplified heterogeneous mechanism [4]. However, this approach uses just volumetric chemical reactions where the detail of surface coverages are missing. This implies an intrinsic approximation of the model response. Even if the porous medium approach gives a good approximation in the catalytic matrix, several works [5] [6] [7] highlighted the influence of three-dimensional flow field on the performance of catalysts due to the presence of the inlet diffuser and the outlet nozzle. Štěpánek et al. [8] coupled the non reactive three dimensional flow field through the monolith with a one-dimensional channel model for the chemical solution. The CFD software transposes pressure, gas flow and temperature profile, within each time step, into the 1D channel model to solve the chemical behaviour along each monolith channel. Recently, a numerical approach for the solution of Navier-Stokes equations applied to arbitrary geometries for reactive flows in heterogeneous systems is proposed [9] [10]. Hence, in order to improve the accuracy of the numerical modelling of a real automotive catalyst, we propose, in this paper, a mixed PFR-CFD model. Moreover, the CFD includes a multi-zones technique to solve the Unsteady Reynolds Averaged Navier-Stokes (URANS) equations in the inlet and outlet ducts and the Navier-Stokes equation considering a porous medium approach in the catalytic matrix. The paper is structured as follows: in the first part, the validation of the coupling of the chemical model with the three dimensional solution proposed. In particular, the consolidated kinetic mechanism proposed by Olsson et al. [11] for the NO_x oxidation and storage process on Pt/BaO support is implemented. Then, a real automotive catalyst has been simulated in unsteady condition comparing the results with the measurements of an experimental test.

2. Numerical Model

2.1. Flow field evaluation

The computational domain of the NO_x Storage Converter used in this work has been obtained by a reverse engineering process on a real commercial device. In Fig. 1 the schematic of the catalytic converter has been reported whereas its main dimensions are listed.

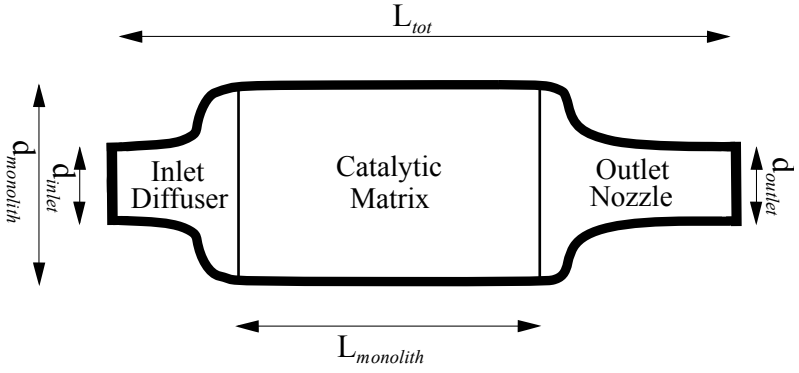

Dimensions	[mm]
L_{tot}	486
$L_{monolith}$	221
d_{inlet}	59
d_{outlet}	57
$d_{monolith}$	152

Fig. 1: Schematic of the catalytic converter. The main dimensions are reported.

The reactive flow field in the catalyst was simulated by means of the ANSYS Fluent CFD code. The flow within the inlet diffuser and the outlet nozzle has been modelled according to the Reynolds Averaged Navier Stokes equations in the hypothesis of unsteady, turbulent flow. The gas mixture is ideal and incompressible, due to the small value (less than 0.1) of the Mach number. The density and viscosity variations due to the mixture composition and the flow

temperature are taken into account in the simulation. The basic equations that are solved are: the continuity equation (1), the momentum equation (2) and the energy equation (3).

$$\frac{\partial \rho}{\partial t} + \nabla \cdot (\rho \vec{v}) = 0 \tag{1}$$

$$\frac{\partial}{\partial t}(\rho \vec{v}) + \nabla \cdot (\rho \vec{v}\vec{v}) = -\nabla p + \nabla \cdot \overline{\overline{\tau}} + \overline{F} \tag{2}$$

$$\frac{\partial}{\partial t}(\rho E) + \nabla \cdot (\vec{v}(\rho E + p)) = \nabla \cdot (k_{eff} \nabla T - \sum_j h_j \vec{J_j} + (\overline{\overline{\tau}}_{eff} \cdot \vec{v})) + S_h \tag{3}$$

where ρ is the mixture density, $\vec{v}$ the flow velocity vector, p the pressure, $\overline{\overline{\tau}}$ the viscous stress tensor, E the total energy of the system, k_{eff} the effective thermal conductivity, $\vec{J_j}$ the diffusion flux of species j and S_h the energy source, which includes the heat involved in the chemical reactions. $\overline{F}$ represents a momentum source term due to the porous medium approximation, modeled according to equation (4)

$$F_i = -\left(\sum_{j=1}^{3} D_{i,j} \mu v_j + \sum_{j=1}^{3} C_{i,j} \frac{1}{2} \rho |v| v_j \right) \tag{4}$$

where D and C are the viscous resistence matrix and the inertial resistence matrix, respectively. The diffusion flux of species j, $\overrightarrow{J_j}$, due to the gradients of concentration and temperature, is defined as follows

$$\overrightarrow{J_j} = -\rho \gamma_{j,m} \nabla Y_j - \gamma_{T,i} \frac{\nabla T}{T} \tag{5}$$

where $\gamma_{i,m}$ is the mass diffusion coefficient for species i and $\gamma_{T,i}$ is the thermal diffusion coefficient. For the gas mixture, the transport equation of the k-th mass fraction, Y_k, has been considered in the form:

$$\frac{\partial \rho Y_k}{\partial t} + \frac{\partial}{\partial x_i}\left(\rho v_i Y_k - \gamma_k \frac{\partial Y_k}{\partial x_i} \right) = S_{Y_k} \tag{6}$$

in which γ_k is the diffusion coefficient and S_k the source term of the species k.

The standard k-ε turbulence model with a standard near wall function [13] has been considered for turbulence closure inside both the inlet diffuser and the outlet nozzle, whereas the porous medium condition with laminar flow has been applied to the region of the catalytic matrix. The three dimensional computational domain is discretized by means of a structured multiblock mesh with 819840 cells. The dimension of the boundary cells of the inlet diffuser and the outlet nozzle has been set to $y^+ \sim 15$ according to the standard near wall function requirement [13]. Being the geometry cylindrical, an O-RING mesh type has been used to avoid singularity at the axis. Each numerical simulation takes about 170 machine-hours in parallel over 8 core of an Intel® Xeon® CPU E5-4620 @ 2.2GHz.

2.2. Chemical Modelling

In the present work, a mean-field heterogenoeus kinetic model is considered so no volumetric reactions are involved. For the generic r-th reversible surface reaction, the reaction rate is

$$\mathcal{R}_r = k_{f,r} \prod_i^{N_g} [G_i]_{wall}^{g'_{i,r}} \prod_i^{N_s} [S_j]_{wall}^{s'_{j,r}} - k_{b,r} \prod_i^{N_g} [G_i]_{wall}^{g''_{i,r}} \prod_i^{N_s} [S_j]_{wall}^{s''_{j,r}} \tag{7}$$

where $[]_{wall}$ represents molar concentrations of surface absorbed gas species, $[G_i]$ and the site species $[S_i]$, $k_{f,r}$ and $k_{b,r}$ represent, respectively, the forward and the backward rate constants for reaction r. The site coverage dependency is taken into account by means of an Arrhenius expression

$$k_{f,r} = A_r T^{\beta_r} e^{\frac{-E_{a,r}}{RT}} \prod_i (10^{Z_i \eta_{i,r}})(Z_i^{\mu_{i,r}})(e^{\frac{-\varepsilon_{i,r} Z_i}{RT}}) \tag{8}$$

where A_r is the preexponential factor, $E_{a,r}$ is the activation energy, β_r the temperature exponent, $\varepsilon_{i,r}$ the activation energy linearly dependent from the fraction of surface site covered by species i, Z_i, defined as

$$Z_i = \frac{[S_i]}{\Gamma} \tag{9}$$

in which Γ represents the surface site density. The mass flux of each species due to convection and diffusion either to or from the surface is weighted with its rate of production or consumption on the surface,

$$\rho_{wall}\gamma_i \frac{\partial Y_{i,wall}}{\partial n} = M_{w,i}\hat{R}_{i,gas} \tag{10}$$

$$\Gamma \frac{\partial Z_i}{\partial t} = \hat{R}_{i,site} \tag{11}$$

where $\hat{R}_{i,gas}$ and $\hat{R}_{i,site}$ are the net molar rates of either production or consumption, respectively, for gas phase and surface-absorbed species defined as

$$\hat{R}_{i,gas} = \sum_{r}^{N_{reaction}} (g''_{i,r} - g'_{i,r})\mathcal{R}_r \tag{12}$$

$$\hat{R}_{i,site} = \sum_{r}^{N_{reaction}} (s''_{i,r} - s'_{i,r})\mathcal{R}_r \tag{13}$$

2.3. NO_x Oxidation-Storage kinetic model

The kinetic scheme used for the NO_x storage and oxidation process has been presented by Olsson et al. [11] and contains five different reversible reactions, summarized in Table 1. The global reaction considers three moles of NO_2 stored on the barium oxide to form barium nitrate ($Ba(NO_3)_2$) with release of one mole of nitrite oxide NO. The model for the storage process is shown in Table 1.

Table 1: Storage process reaction scheme

R1	$NO_{2(g)} + BaO$	$\Longleftrightarrow$	$BaO–NO_2$
R2	$BaO–NO_2$	$\Longleftrightarrow$	$BaO–O+NO_{(g)}$
R3	$NO_{2(g)}+BaO–O$	$\Longleftrightarrow$	$BaO–NO_3$
R4	$NO_{2(g)}+BaO–NO_3$	$\Longleftrightarrow$	$Ba(NO_3)_2$
R5	$2BaO–O$	$\Longleftrightarrow$	$2BaO + O_{2(g)}$

In this work the NO_x oxidation mechanism on Pt is coupled to the storage model on BaO. This mechanism views four reversible reactions involving $NO - NO_2$ over the Pt sites and the oxidation of nitrite oxide to nitrite dioxide through a Langmuir-Hinshelwood model [14], in which two molecules reacting in heterogeous catalysis have to be first absorbed by the superficial catalytic sites. The kinetic scheme is shown in Table 2.

Table 2: Oxidation process reaction scheme

R6	$O_{2(g)} + 2Pt$	$\Longleftrightarrow$	$2O–Pt$
R7	$NO_{(g)} + Pt$	$\Longleftrightarrow$	$NO–Pt$
R8	$NO_{2(g)} + Pt$	$\Longleftrightarrow$	$NO_2–Pt$
R9	$NO–Pt+O\text{-}Pt$	$\Longleftrightarrow$	$NO_2–Pt+Pt$

The coupling of this two subset of kinetic reactions acting on two different sites [11] needs the presence of the spillover mechanism between platinum and barium oxide, described by the two reversible reactions shown in Table 3.

Table 3: Spillover process reaction scheme

R10	$NO_2–Pt$	$\Longleftrightarrow$	$NO_{2(g)}^{<2nd>}+Pt$
R11	$Ba(NO_3)_2$	$\Longleftrightarrow$	$NO_{2(g)}^{<2nd>}+Pt$

The simple implementation of the default mean values presented by Olsson et al. [11] did not allow a correct description of the phenomenon, so we needed to proceed with a tuning inside the available range of some parameters during the validation process. The kinetic parameters used in the simulation, considering the barium oxide site density as $\Gamma_{BaO} = 8.3768 \cdot 10^{-6} \frac{kmol}{m^2}$ and the platinum site density $\Gamma_{Pt} = 1.1333 \cdot 10^{-8} \frac{kmol}{m^2}$ are reffered to those exposed in Olsson et al. [11] with some adjustement within the confidence interval on two activation energy values. The spillover reversible reaction has been modeled considering a fictitious nitrogen dioxide volumetric species ($NO_{2(g)}^{<2nd>}$) which spills over from platinum sites to $BaO - NO_3$ to form barium nitrate $Ba(NO_3)_2$. Reactions $R4_b$, $R6_b$, $R8_b$, $R10_f$ and $R11_f$, due to repulsive interactions by the species involved, view an activation energy dependent from the surface coverage as exposed by Olsson et al. [11].

3. Validation of the coupled kinetic model

The implementation of the chemical reactions in the CFD software went through a validation process of the kinetic model. After having rebuilt the experimental setup used in the work of Olsson, simulations have been carried out in a single channel and then on the entire catalyst with the matrix zone simulated as a porous zone. The same approach was used in a previous work [12]. The catalyst used by Olsson et al. [11] to develop the chemical model is a monolith with 69 square channels, about 1mm for each side and a length of 15mm. The entire catalyst was simulated by directly solving the Navier-Stokes equations considering the reactive monolith as a porous medium; without any turbulence model due to the low Reynolds Number registered inside the channel (Re ≅ 13). Fig. 2 shows the images of the mesh for the channel and the entire catalyst. In Fig. 3 it is possible to see the two graphics for the validation experience. It is worth noting that imposing 680 ppm of nitrite dioxide (NO_2) in nitrogen (N_2) at 350 [°C] simulations on the entire catalyst and the single channel results agree well with the experimental data with a deviation less then 3%. Good results are shown also imposing 600 ppm of nitrite oxide (NO) in nitrogen (N_2) at 350 [°C]. However, when the temperature ramp begins, there are differences with the results presented by Olsson et al. [11]. The current research activity is aimed at solving this difference.

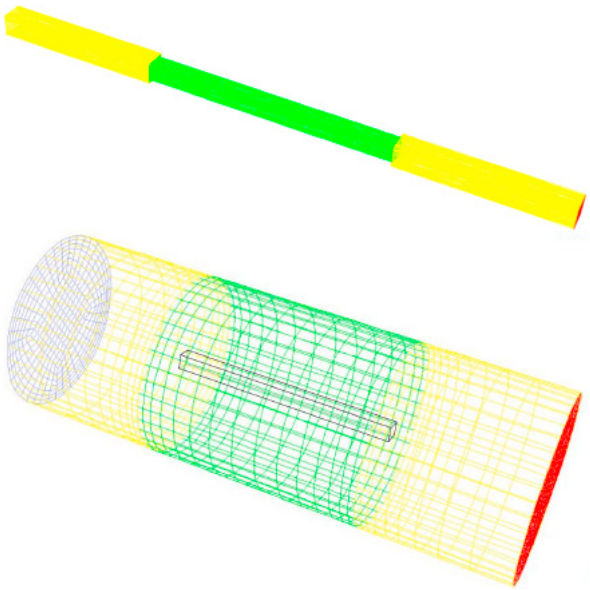

Fig. 2: Images of the mesh for the entire catalyst and the single channel used for the validation process.

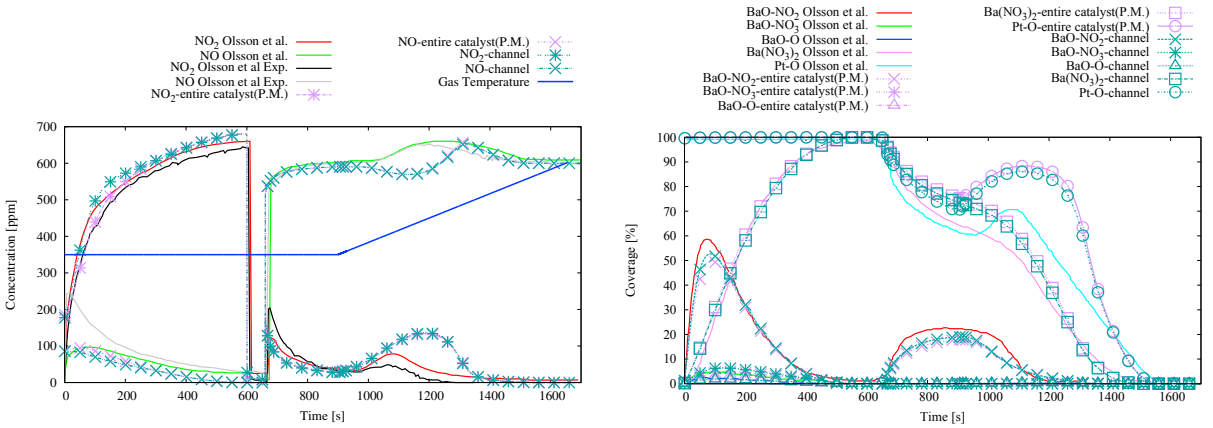

Fig. 3: Validation process for the Oxidation-Storage model (P.M. stands for Porous Medium). On the right hand side: volumetric quantities are shown compared with the numerical and experimental results presented by Olsson et al. [11]. On the left hand side: coverage site species compared with the numerical results presented by Olsson et al. [11].

4. Results

Unsteady simulations on a real catalyst are conducted. The NO_x inlet concentration, the flow rate and the temperature are changed during the experiment by means of User Defined Function implemented in Ansys Fluent reproducing the inlet data of the experiment. In this case the barium-oxide and the platinum site densities are imposed equal to Γ_{BaO}=1.6754e-04 kmol/m^2 and Γ_{Pt}=2.2667e-07 kmol/m^2, respectively. The site densities imposed in the model are extrapolated by means of a numerical test. Due to the unsteadyness of the test, averaged values of simulated quantities are shown in Table 4.

Table 4: Main characteristic quantities of the experimental test here reproduced. Time averaged values over 100s are reported.

Flow Rate [kg/s]	0.055
Temperature$_{inlet}$ [°C]	336
Temperature$_{outlet}$ [°C]	334
$C_3H_{6(inlet)}$ [ppm]	5.55
$CO_{2(inlet)}$ [ppm]	77196.8
$CO_{(inlet)}$ [ppm]	1.4
$H_2O_{(inlet)}$ [ppm]	75697.4
$N_{2(inlet)}$ [ppm]	760200
$NO_{(inlet)}$ [ppm]	58.3
$NO_{2(inlet)}$ [ppm]	57.4
$O_{2(inlet)}$ [ppm]	86783.3

In Fig. 4, on the left hand side, the inlet and outlet NO_x concentrations are reported for both numerical and experimental measurements. The overall abatement is correctly reproduced, in particular, the NO_x abatement is the 98.9% for the experiment and 94.8% for the numerical model. On the right hand side of Fig. 4 only the outlet NO_x is compared between the experiment and simulation. It is recognized a fairly good agreement between the numerical and experimental NO_x abatement. The outlet concentration of the NO_x of the model are slightly higher, but can be further diminished increasing the site density imposed. It is worth noting a dumping in the outlet NO_x with respect to the inlet oscillations that depends on the concentration of BaO in the washcoat. Even this phenomenon suggests to increase the site density of BaO of the model. Indeed, the higher is the BaO concentration in the washcoat, the greater is the adsorption velocity of NO_x. Thus, the inlet peaks of NO_x could be dumped. Fig. 5 shows the temperature behaviour of the numerical model with respect to the experimental results. The outlet temperature has a good agreement with the experimental measurements confirming the reliability of the mixed PFR-CFD model here proposed.

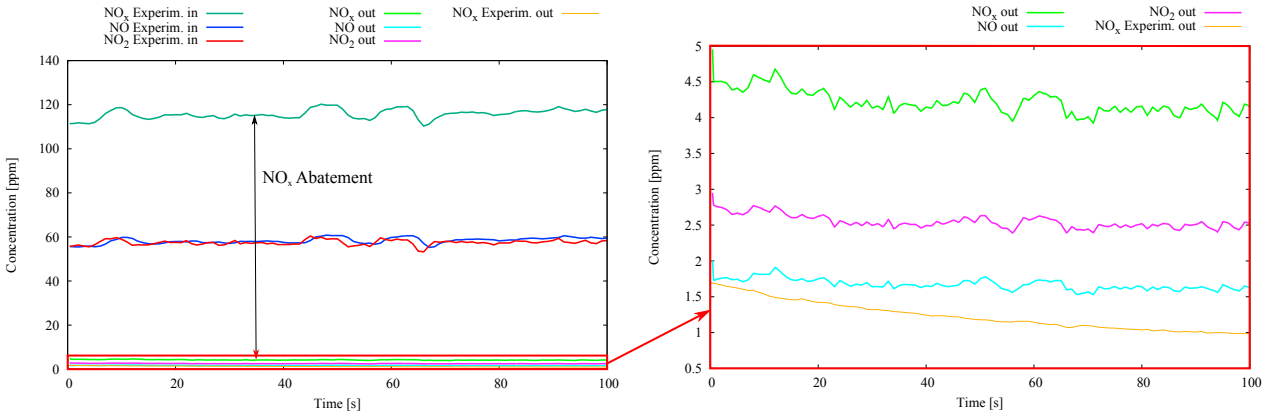

Fig. 4: Time series of the volumetric NO, NO_2 and the total NO_x concentrations of numerical and experimental test. On the left hand side: inlet and outlet measures. On the right hand side: rescaled comparison of the outlet concentrations.

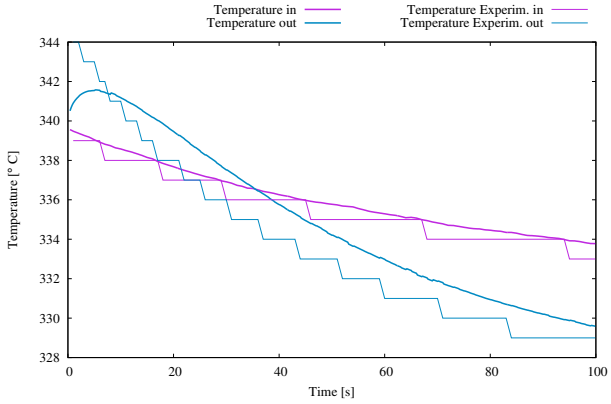

Fig. 5: Comparison of the time series of the inlet/outlet catalyst temperature between experimental and numerical test.

From NO and NO_2 spatial distributions shown in Fig. 6 at time 40s it is evident their three-dimensional character. Recirculation zones at the inlet of the catalytic matrix generate an irregular flow field that affects the efficiency of the catalytic conversion along the radial direction. Therefore, through the axial zone of the catalyst matrix a greater flow rate of exhaust brings to a higher space velocity.

5. Conclusions

In this work, a mixed PFR-CFD model for the simulation of a real LNT automotive catalyst has been proposed. The geometry considered has been derived from a commercial device. The CFD includes a multi zones approach where URANS and porous medium governing equations are implemented for inlet/outlet ducts and catalyst matrix, respectively. Recirculation zones are predicted in the inlet diffuser. They induce a non-homogeneous distribution of the inlet flow rate in the active matrix. This determines a non-uniform space velocity distribution inside catalytic matrix. The views of the concentration contours of NO_x support this finding. This phenomenon, not particularly critical for this axis-symmetric configuration, it could be greately amplified when real exhaust system ducts (with extreme complex paths rich of elbows and curves) are considered. For this reason, in the next future, these complex configurations will be investigated. The PFR model includes a detailed mechanism with superficial reactions associated to the catalyst matrix. The chemical model has been detailed by means of 22 reactions where the kinetic parameter are validated according to the literature. The chemistry includes adsorption, desorption of the volumetric species, only surface reactions on the same site and mutual interactions between heterogeneous active sites (spillover). The comparison

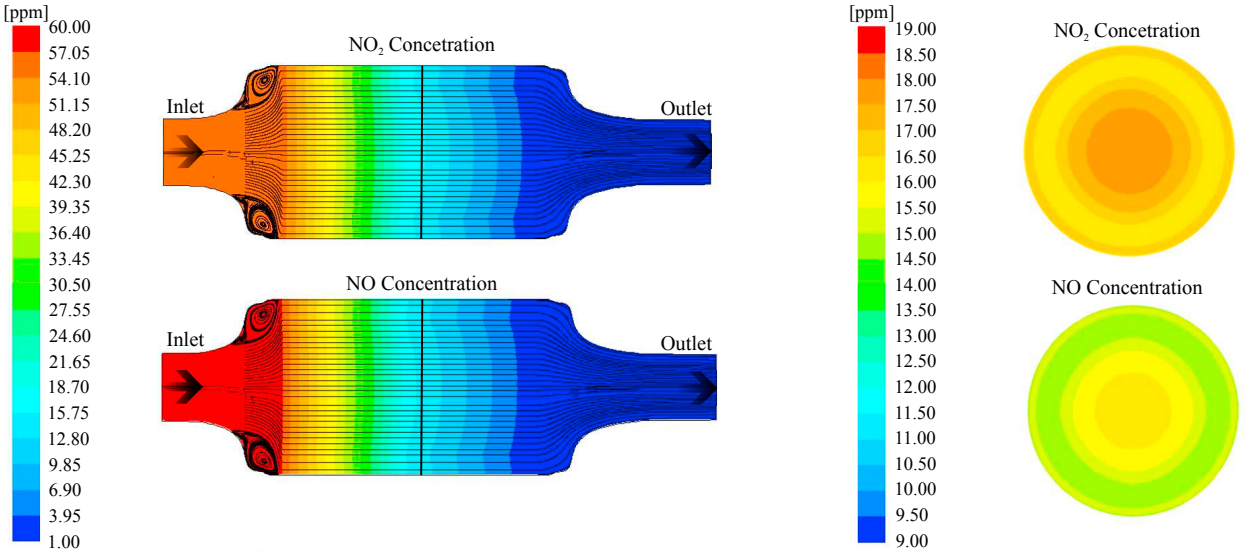

Fig. 6: Volumetric concentration of NO and NO_2 into the catalyst expressed in [ppm]. On the left hand side: spatial distribution on a lateral section of the catalyst of NO_2, on the upper side, and NO, on the bottom side. On the right hand side: spatial distribution in a center cross section of the catalyst with a different legend scale to take account of little concentration variation, for NO_2, on the upper side, and NO, on the bottom side.

between experimental measurements and the present numerical results are in fairly good agreement and confirms the reliability of the model here proposed.

References

[1] R. S. Larson and V. K. Chakravarthy and J. A. Pihl and C. Stuart Daw. (2012) "Microkinetic modeling of lean NO_x trap chemistry", *Chemical Engineering Journal* 189 (2012): 134–147.

[2] A. S. Kota and D. Luss and V. Balakotaiah (2015) "Micro-kinetics of NO_x storage and reduction with $H_2/CO/C_3H_6$ on $Pt/BaO/Al_2O_3$ monolith catalyst", *Chemical Engineering Journal* 262 (2015): 541–551.

[3] S.F. Benjamin and C.A. Roberts (2007) "Three-dimensional modelling of NO_x and particulate traps usng CFD: A porous medium approach", *Applied Mathematical Modelling* 31 (2007): 2446–2460.

[4] F. Laurent and C.J. Pope and H. Mahzoul and L. Delfosse and P. Gilot (2003) "Modelling of NO_x adsorption over NO_x adsorbers", *Chemical Engineering Science* 58 (2003): 1793–1803.

[5] S. J. Jeong (2014) "A full transient three-dimensional study on the effect of pulsating exhaust flow under real running condition on the thermal and chemical behavior of closed-coupled catalyst", *Chemical Engineering Science* 117 (2014): 18–30.

[6] A. Algeri and S. Bova and C. De Bartolo and A. Nigro (2011) "Numerical and experimental analysis of the flow field within a lean NO_x trap for diesel engine", *SAE Technical Paper 2011* (2011).

[7] G. Agrawal and N. S. Kaisare and S. Pushpavanam and K. Ramanathan (2012) "Modeling the effect of flow mal-distribution on the performance of a catalytic converter", *Chemical Engineering Science* 71 (2012): 310–320.

[8] J. Štěpánek and P. Kočí and M. Marek and M. Kubíček "Catalyst simulation based on coupling of 3D CFD tool with effective 1D channel models", *Catalysis Today* 188 (2012): 87–93

[9] M. Maestri and A. Cuoci "Coupling CFD with detailed microkinetic modeling in heterogeneous catalysis", *Chemical Engineering Science* 96 (2013): 106–117

[10] M. Corbetta and F. Manenti and C. G. Visconti "CATalytic - Post Processor (CAT-PP): A new metodology for the CFD-based simulation of highly reactive heterogeneous system", *Computer and Chemical Engineering* 60 (2014): 76–85

[11] L. Olsson and H. Persson and E. Fridell and M. Skoglundh and B. Andersson (2001) "A Kinetic Study of NO Oxidation and NO_x Storage on Pt/Al_2O_3 and $Pt/BaO/Al_2O_3$", *Journal Phisical Chemistry B* 105 (2001): 6895–6906.

[12] F. Fornarelli and S. M. Camporeale and R. Dadduzio and B. Fortunato and M. Torresi (2015) "Numerical simulation of the flow field and chemical reactions within a NSC diesel catalyst", *Energy Procedia* 82 (2015): 381–388.

[13] "ANSYS Fluent Academic Research, Release 17.2, Theory Guide", *ANSYS, Inc.*.

[14] M. E. Bartram and R. G. Windham and B. E. Koel (1988) "Coadsorption of Nitrogen Dioxide and Oxygen on Pt(111)", *Langmuir* 4 (1988): 240–246.